Original Research Article

Calculation of Cohesive Energies of 3-D Bismuth Selenide (Bi_2Se_3) and Bismuth Antimony BiSb Topological Insulators: DFT study

Abstract

The cohesive energies of 3-dimensional (3-D) topological insulators bismuth antimony (BiSb) and bismuth selenide (Bi_2Se_3) were calculated. The Fritz Haber Institute Ab-initio molecular simulations (FHI-aims) code was employed for this calculation. The output files of the FHI-aims code were used during the computation and the total energies at each number of iterations for single free atoms and bulk were then calculated. The results from this work revealed that bismuth atom becomes stable at 3rd iteration meanwhile both selenium and antimony atoms gain stability at the 5th iteration. The results also showed that bismuth antimony acquire stability at the 3rd iteration and bismuth selenide gain stability at 9th iteration. This implies that among the free atoms studied in this work bismuth atom is more stable and for the bulk bismuth antimony is more stable. The cohesive energies of BiSb and Bi_2Se_3 were calculated using the optimized parameters. The results obtained from this work compared reasonably well with experimental results and have little percentage errors of 1.30% for bismuth antimony and 29.55% for bismuth selenide. The deviation observed in this work may be due to the DFT calculation of the solid rather than the atoms themselves.

Keywords: Cohesive Energies; Topological Insulator; FHI-aims,

1. INTRODUCTION

The electrical conductor, insulator, semiconductor, and the superconductor were the first electronic phase of matter to be defined. Recent work has, however, discovered a new electronic phase called a topological insulator. The most exciting thing about this new electronic phase is the behaviour. Materials in this new phase behave strangely. The topological insulator can insulate on the inside but conduct on the outside. This new electronic phase of matter are said to be materials with non-trivial symmetry protected topological order that behaves as an insulator in its interior but whose surface contains conducting states [1]. The materials in this phase are unique in the sense that the conducting electrons arrange themselves into spin-up electrons travelling in one direction, and spin-down electrons travelling in the other. This imply that electrons can only move along the surface of the material.

The conducting surface possessed by topological insulator is however not unique to them only, ordinary band insulators also support conductivity on the surface states. The only distinctive thing about topological insulators is that their surface states are symmetry protected by particle number of conservation and time reversal symmetry [2-4].

In the bulk of a non-interacting topological insulator, the electronic band structure resembles an ordinary band insulator, with the Femi level falling between the conduction and valence bands. On the surface of a topological insulator there are special states that fall within the bulk energy gap and allow surface metallic conduction. Carriers in these surface states have their spin locked at a right-angle to their momentum (spin-momentum locking). At a given energy the only other available electronic states have different spin, so the U-turn scattering is strongly suppressed and conduction on the surface is highly metallic. Non-interacting topological insulators are characterized by an index known as the Z_2 topological invariants similar to the genus in topology [5].

The protected conducting states in the surface are required by time-reversal symmetry and the band structure of the material. The states cannot be removed by surface passivation if it does not break the time-reversal symmetry, which does not happen with potential or spin-orbit scattering but happens in case of true magnetic impurities such as spin- scattering [6].

Topological insulators have a rather unusual history because unlike almost every other exotic phase of matter, topological insulators were characterized theoretically before being discovered experimentally. This new electronic phase of matter was discovered in 2007 experimentally. The first

realized 3D topological state (symmetry-protected surface states) discovered experimentally in bismuth-antimony (BiSb) [7]. Shortly thereafter symmetry-protected surface states were discovered in pure antimony (Sb), bismuth selenide (Bi_2Se_3), bismuth telluride (Bi_2Te_3) and antimony telluride (Sb_2Te_3) [8].

Today, many semiconductors within the large family of Heusler materials are now believed to exhibit topological surface states [9]. In some of these materials Femi level actually falls in either the conduction or valence bands due to naturally occurring defects and must be pushed into the bulk gap by doping or gating [10].

This recent discovery did draw the attention of many Solid-State Physicists. A related topological property known as the quantum Hall effect had already been found in 2D ribbons in the early 1980s but the discovery of the first example of a 3D topological phase reignited that earlier interest. Given that the 3D topological insulators are fairly standard bulk semiconductors and their topological characteristics can survive to high temperatures [11]. Other notable research on topological insulators is in energy generation of electricity by converting thermal gradients occurring naturally or from waste heat sources into useful electrical energy [12] and Raman Spectroscopy determination of Debye temperature and atomic cohesive energy [13]. In this work however, the researchers intend to calculate the cohesive energies of bismuth selenide (Bi_2Se_3) and bismuth antimony (BiSb) using density functional theory.

Cohesive energy is amount of energy involved when a crystalline solid is formed from infinity separated atoms or the amount of energy required to separate atoms in a crystalline solid to infinite distance. In Physics however, cohesive energy means the difference between the average energy of the free atoms and that of the atoms of a solid especially a crystal. It is the quantity which determines the structure, because different possible structures would have different cohesive energies [14]. The magnitude of cohesive energy also tells us about the stability and chemical reactivity of solids.

2. THEORETICAL FRAMEWORK

Density Functional Theory (DFT) is a computational quantum mechanical modelling method used in Physics, Chemistry and material science to investigate the electronic structure (especially the ground state) of many-body systems, in particular atoms, molecules, and the condensed phase. Applying this theory, the properties of a many-electron, which in this case is the spatially dependent electron density. DFT has been the dominant method for quantum

mechanical simulation of periodic systems. In recent years it has also been adopted by quantum chemistry and is now very widely used for simulation of energy surfaces in molecules [15].

Traditional methods in electronic structure theory, particularly the Hatree-Fock theory and its descendants are based on the complicated many-electron wave function. The main objective of DFT is to replace the many-body electronic wave function with the electronic density as the basic quantity. Thereby making many-body wave function dependent on 3N variables, three special variables for each of the N electrons, the density is only a function of the three variables and is simpler to deal with both conceptually and practically [16].

2.1. The Hohenberg-Kohn Theorem

The Hohenberg –Kohn (H-K) theorem states that the electrons density of any system determines all ground-state properties of the system. In this case the total ground state energy of a many-electron system is a function of the density.

The theory assumes a system of N-interacting electrons under an external potential $V(r)$. This potential is usually the coulomb potential of the nuclei. If the system has a non-degenerate ground state, it is obvious that there is only one ground state charge density that corresponds to a given $V(r)$. Hohenberg and Kohn demonstrated that there is only one external potential $V(r)$ that yields a given ground state charge density $n(r)$.

Hohenberg and Kohn demonstrated that for many-electron Hamiltonian $H = T + U + V$, with ground state wave function, ψ. Whereas T, U, V are the kinetic energy, electron-electron interaction and the external potential respectively. The charge density $n(r)$ is defined by:

$$n(r) = N \int \left|\psi\left(r_1, r_2, r_3 \ldots r_N\right)\right|^2 dr^2 . dr^N \qquad (1)$$

Differentiating the Hamiltonian $H' = T' + U' + V'$. The potential V and its derivatives V' does not differ by a constant. That is to say $V - V' \neq$ constant with the ground state wave function ψ.

Assuming that the ground state charge densities are the same (i.e. $n[V] = n'[V']$. The following inequality will hold [17-18].

$$E < \langle\psi'|H|\psi'\rangle = \langle\psi'|H'|\psi'\rangle + \langle\psi'|H - H'|\psi'\rangle \qquad (2)$$

$$E < E' + \langle\psi'|T + U + V - T - U - V'|\psi' \qquad (3)$$

This implies that

$$E < E' + \int n(r)\{V - V'\}dr \quad (4)$$

The reverse relation of equation (4) will now be

$$E' < E - \int n(r)\{V - V'\}\,dr \quad (5)$$

Adding equation (4) and equation (5) gives

$$E + E' < E' + E \quad \text{Contradiction!} \quad (6)$$

The inequality in the above equation is strict because ψ and ψ' are different, being eigen state of different Hamiltonian. Reversing the prime and unprime quantities, one obtain an inconsistent result. This showed that no two potentials can have the same density. The first Hohenberg-Kohn theorem that has a straight forward consequence is that of the ground state energy E. The theory also uniquely determined by the ground state charge density. It is a function of density $E[n(r)]$ [19] and can be written mathematically as:

$$E[n(r)] = (\psi|T + U + V|\psi) = (\psi[T + U]\psi) + (\psi|V|\psi) = F[n(r)] + \int n(r)V(r)dr \quad (7)$$

$F[n(r)]$ is a universal function of the charge density $n(r)$ but not of $V(r)$ also known as the H-K functional [20]. For this functional variation principle holds and the ground state energy is minimized by the ground state charge density. In this way, the DFT exactly reduces the N-body problem to determine a 3-dimensional function $n(r)$ which minimizes a functional $E[n(r)]$.

2.2. The Kohn-Sham (KS) Equations

Kohn and Sham in 1965 reformulated the problem in a more familiar form and opened up the practical application of DFT. Here, the system of interacting electrons is mapped onto a fictitious system of non-interacting electrons having the same charge density $n(r)$. K-S represented the ground state energy charge density by a system of non-interacting electrons over one-electron orbitals also known as K-S orbitals ψ_i as:

$$n(r) = 2\sum_i |\psi_i(r)|^2 \quad (8)$$

Where i runs from 1 to $\frac{N}{2}$. If we assume a double occupancy of all states and Kohn-Sham orbitals are solutions to the Schrodinger equation

$$E_i\psi_i(r) = \left(-\frac{\hbar^2}{2m}\nabla^2 + V_{ks}(r)\right)\psi_i(r) \quad (9)$$

Where m is the electron mass. Obeying orthogonality constraints we write:

$$\int \psi_i^*(r)\psi_j(r)dr = \delta_{ij} \quad (10)$$

The existence of a unique potential $V_{ks}(r)$ having $n(r)$ as its ground state charge density is a consequence of the Hohenberg and Kohn theorem which holds irrespective of the form of the electron-electron interaction U.

3. METHOD

The main task in the DFT method is the computation of the total energy and derived quantities of molecules and solids of condensed matter in its electronic ground state [21]. To calculate the cohesive energies of bismuth selenide and bismuth antimonite, the ground state total energies of Bi, Se, and Sb for single free atom and bulk were calculated first. The energies were then converted to cohesive energies of Bi_2Se_3 and BiSb using the equation below:

$$E_{coh} = \frac{E_{bulk} - NE_{atom}}{N} = -\left[\frac{E_{bulk}}{N} - E_{atom}\right] \quad (11)$$

The calculations were carried out using FHI-aims code upgrade 6 version 071711_6. The code works on any Linux operating system. The computation can only be done after building an executable binary file. The FHI-aims package is distributed in a source code form and requires a working Linux based operating system (Ubuntu 11.10 in this case). The code also require a working FORTRAN 95 (or later) compiler. In this work, a × 86 type computer and an Intel's ifort (specifically composerxe 2011.6.233) was installed. The compiler version of laplack library, and a library providing optimized basic linear algebra subroutines (BLAS). Standard labraries such as Intel's mkl or IBM's essl provide both lapack and BLAS support. Intel's composerxe 2011.6.233 comes with mkl.

The FHI-aims requires two input files (i.e., control.in that contains all runtime-specific information and geometry. It also contains information directly related to the atomic structure for a given calculation). The two input files must be place in the same directly from where the FHI-aims binary file is invoked at the terminal. All necessary adjustment were made for building the executable binary file for the running of the code and the program was successfully build.

4. RESULTS AND DISCUSSION

The output files of the FHI-aims code were used to obtain the results for this work. The total energies and the number of iterations for single free atoms and bulk were obtained in this work. The graphs of total energies against the number of iterations were plotted in order to obtain the optimized parameters for HCP (Bi, Se, and Sb) lattices within the local density approximation (LDA). The cohesive energies of Bi_2Se_3 and BiSb were then calculated using the optimized parameters. The results obtained from this work are presented below:

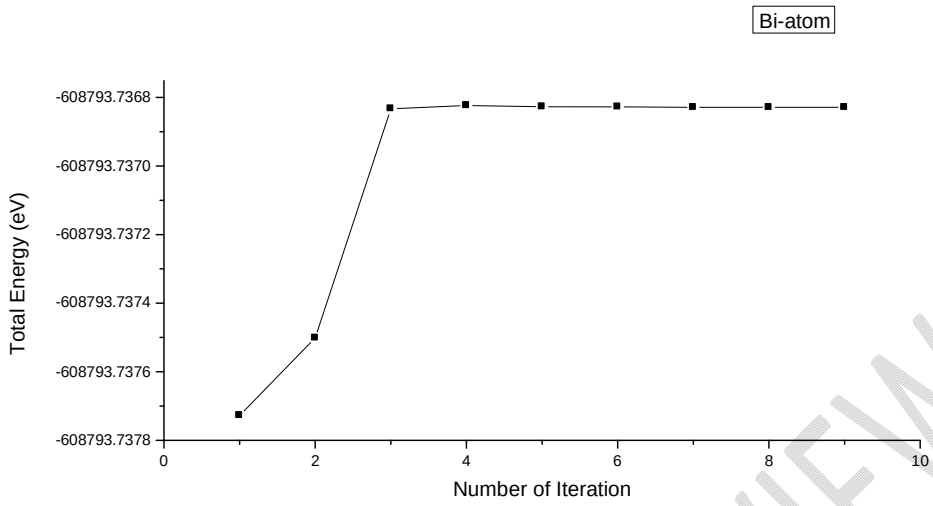

Figure 1 : Bismuth (Bi) binding curve for total energy against the number of iteration. The figure above showed that the total energy of bismuth atom became stable at the 3rd iteration.

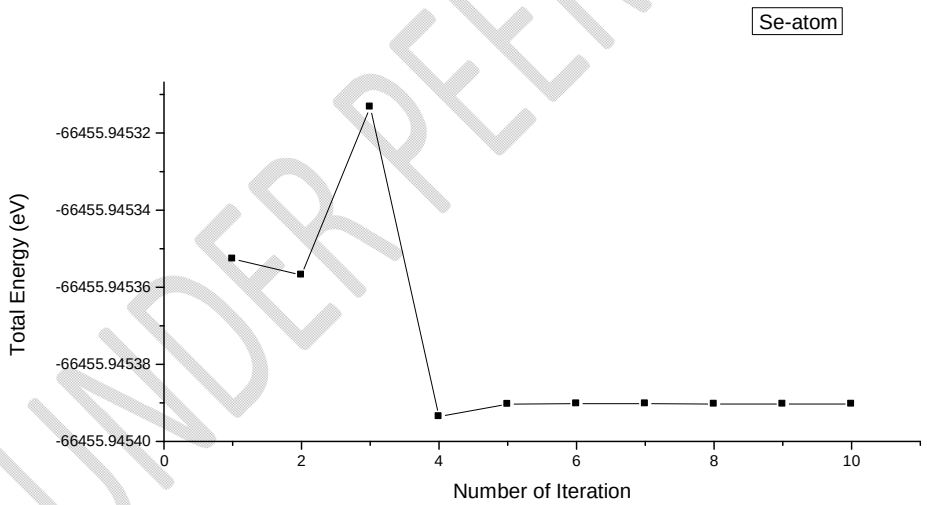

Figure 2: Selenium (Se) binding curve for total energy against the number of iterations. The above graph showed that the total energy of selenium atom gain stability at the 5th iteration

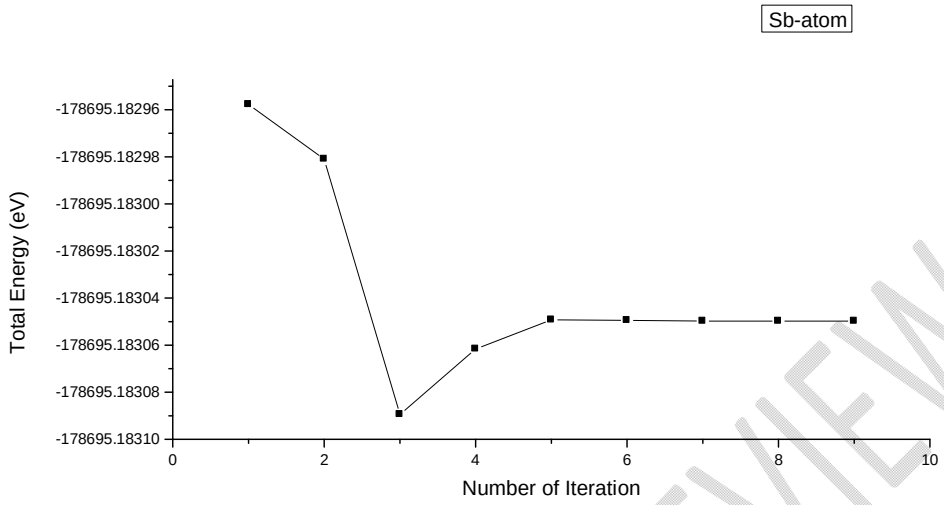

Figure 3: Antimony (Sb) binding curve for total energy against the number of iterations. This figure showed that the total energy of antimony atom becomes a bit stable at the 5th iteration.

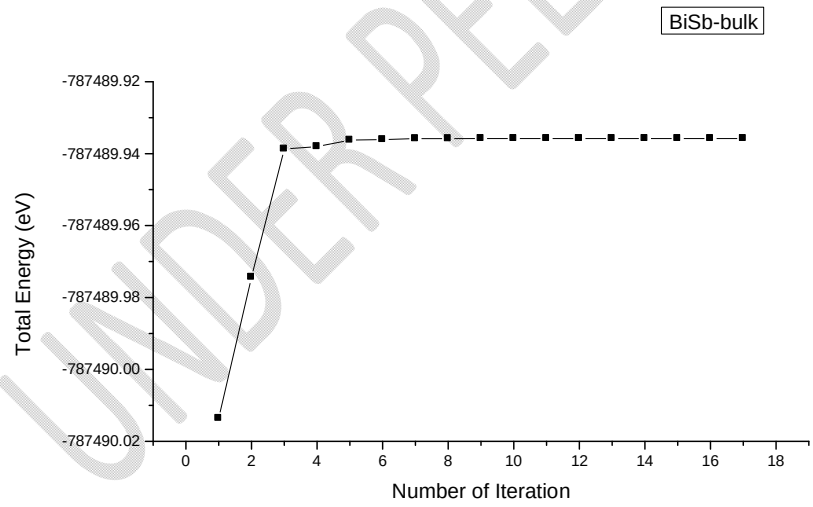

Figure 4: Bismuth antimonite (BiSb) binding curve for total energy against the number of iterations. The binding curve for the total energy showed that bismuth antimonite (bulk) is stable at the 3th iteration.

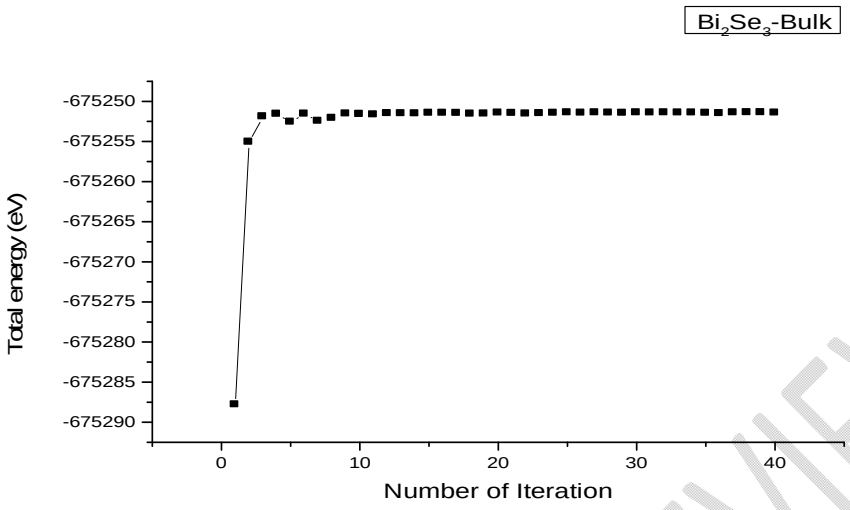

Figure 5: Bismuth selenide (Bi_2Se_3) binding curve for total energy against the number of iterations. The total energy of antimony telluride become stable at the 9th iteration.

The binding energy curve for single free atoms of Bi, Se, and Sb shown in figure 1 to 3 showed that the total energy of bismuth atom become stable at the 3rd iteration but selenium, and antimony atoms gain their stability at the 5th iteration. This showed that the total energy of bismuth atom converges faster than that of Se, and Sb atoms. The total energy of bismuth atom acquire stability beginning from 3rd iteration. Meanwhile the total energy of selenium, and antimony atom begin their stability at the 5th iteration.

The cohesive energies of bismuth selenide (Bi_2Se_3) and bismuth antimonite (BiSb) were calculated using the following relations:

$$E_{coh} = E_{tot}(Bi_2 + Se_3) - E_{tot}(Bi_2Se_3)$$

$$E_{coh} = E_{tot}(BiSb) - E_{tot}(BiSb)$$

The cohesive energy of bismuth antimony was calculated to be 1.02eV in this work and that of cohesive energy of bismuth selenide calculated in work is 1.76eV. This result is in reasonable agreement

with the cohesive energy obtained from T-dependent Raman shift method for bismuth selenide which is 1.09eV and 1.24eV respectively [13].

The binding curve for Bi_2Se_3 and BiSb are shown in figures 4 and 5 above. The binding curve in figure 5 showed that the total energy of BiSb becomes stable at 3^{rd} iteration whereas that of Bi_2Se_3 become stable at the 9^{th} iteration see figure 5 above. This behaviour exhibited by bismuth antimonite indicate that the alloy's total energy converges faster than that of bismuth selenide.

Conclusion

The cohesive energies of bismuth antimony and bismuth selenide were calculated within the local density approximation (LDA). The results of the total energy required for separating the condensed compound during the optimized process is found to converge faster with the 12 × 12 × 12 k-grid points in the Brillioun zone of the FHI-aims code. The result presented above have confirmed a faster and more accurate study of the solid considered when compared to literature report of other studies. The values obtained are in agreement with experimental value [13] within some reasonable percentage errors. The calculated cohesive energies for bismuth antimony and bismuth selenide are observe to differ by 1.30% and 29.55% respectively. The major measure source of this deviation may come from the present DFT calculation of the solid rather than the atom.

COMPETING INTERESTS DISCLAIMER:

Authors have declared that no competing interests exist. The products used for this research are commonly and predominantly use products in our area of research and country. There is absolutely no conflict of interest between the authors and producers of the products because we do not intend to use these products as an avenue for any litigation but for the advancement of knowledge. Also, the research was not funded by the producing company rather it was funded by personal efforts of the authors.

REFERENCES

1. Kane. C.L and Mele, E.J. (1468). Z_2 Topological order and the Quantum Spin Hall Effect. *Physical Review Letter.* 9(14): 146802.
2. Zheng-Cheng, G. and Xiao-Gang, W. (2009). Tensor-Entanglement-Filtering Renormalization Approach and Symmetry-Protected Topological order. *Physical Review* B80: 155131.
3. Pollman, F., Berg, E., T., Ari, M., Oshikawa, M. (2012). Symmetry Protection of Topological Phases in one –dimensional quantum spin systems. *Physical Review.* 85(7): 075125.
4. Chen, X., Gu. Z., Wen, X. (2011). Classification of Gapped Symmetry Phases in 1D spin systems. *Physical Review* B83 (3): 035107.
5. Th. Guhr, A., Muller-Groening, H.A., Weiden, M. (1998). Random Matrix Theories in Quantum Physics: Common Concepts. Physics Report Vd. 299: 189-425.
6. Hsieh, D., Dong, Q., Andrew, L.W., Yuq,X., Yusan, H., Robert,. C., Zahid-Hasan, M. (2008). A Topological Dirac insulator in a quantum spin Hall phase .*Nature materials.* 452(9):970-974.
7. Hasan, M.Z., Kane, C.L. (2010). Topological insulators. *Review of Modern Physics.* 82(4): 3045-3067.
8. Chadov, S., Xiao-Liang, Q., Jurgen, K., Gerhard, H.F., Claudia, F., Shou-Cheng, Z. (2010). Tunable Multifunctional Topological Insulators in termary Heusler Compounds. *Nature materials* 9(7): 541-545.
9. Lin, H., Andre-Wray, L., Yuqi, X., Suyan, X., Shuang, J., Robert, J.C., Arun, B., Zahid Hasan, M. (2010). Half-Heusler termary Compounds as new multifunction experimental platforms for Topological quantum Phenomena. *Nature material*. 9(7): 546-549.
10. Hsieh, D., Xia, Y., Qian, D., Wray, L., Meier, F., Dil, J.H., Osterwalder, J., Pathey, L., Fedorov, A.V., Lin, H., Bansil, A. Graver,D., Hor, Y.S.,

Cava, R.J., Hasan, M.Z. (2009). Observation of Time-Reversal-Protected Single-Dirac-Cone Topological-Insulator States in Bi_2Te and Sb_2Te_3.
11. Kane, C and Moore, J. (2014). Topological Insulators. Physics World Archive. IOP Publishing Ltd. ISSN: 0953-8585.
12. Naylor, A.J. (2014). Towards Highly-Efficient Thermoelectric Power Harvesting Gerators. Ph.D. thesis in the Faculty of Natural and Environmental Sciences, School of Chemistry. University of Southampton
13. Yang, X.X., Zhou, Z., Wang, Y., Jiang, R., Zheng, W.T., Sun, C (2012). Raman Spectroscopy Determination of the Debye Temperature and Atomic Cohesive energy of CdS. CdSe, Bi_2Se_3 and Sb_2Te_3 Nanostructure. *Journal of Applied Physics*, 112(8): 0835008.
Physical Review Letters. 103(14): 146401.
14. Verma, A.S., Sarkar, B.K., Jindal, V.K. (2010). Cohesive Energy of Zincblende ($A^{III}B^{V}$ and $A^{II}B^{VI}$) Structured solids. *Pramana Journal of Physics, Indian Academy of Science.* 74(5): 851-855.
15. Abdu, S.G., Adamu, M.A., Onimisi, M.Y. (2018). DFT Computations of the Ground State Energy per Atom of Fullerenes (C_{60}). *Science World Journal*. 13(1): 35-38.
16. Galadanci, G.S.M., Garba, B. (2013). Computation of the Ground State Cohesive Properties of Alas Crystalline Structure Using FHI-aims code. *IOS R-JAP*. 4(5): 85-95.
17. Giannozzi, P. (2005). Density Functional Theory for electronic structure calculations structure della material. 1
18. Sholl, D.S., Steckel, J.A. (2009). Density Functional Theory: A Practical Introduction. John Willey & Sons Inc, Publication.
19. Tuckerman, M. (2004). Introduction to DFT. Maria Currie Tutorial Series. Modelling Biomolecules.
20. Blum, V., Gehrke, R., Hanke, F., Haviu, V., Ren, X., Reuter, K., Scheffler, M. (2009). Ab iniotio molecular simulations with numeric atom-centered orbitals. *Computer Physics communication*. 180: 2175-2196.
21. Mishra, S.K., Satpathy, S. and Jepsen, O. (1997). Electronic Structure and Thermoelectric Properties of Bismuth telluride and Bismuth selenide.
Journal of Physics: Condensed Matter.9: 461-470.